





Article

Low Temperature Plasma Strategies for *Xylella fastidiosa* Inactivation

Paolo Francesco Ambrico ^{1,*}, Stefania Zicca ², Marianna Ambrico ¹, Palma Rosa Rotondo ³, Angelo De Stradis ², Giorgio Dilecce ¹, Maria Saponari ², Donato Boscia ² and Pasquale Saldarelli ^{2,*}

¹ National Research Council of Italy (CNR), Institute for Plasma Science and Technology (ISTP), Via Amendola 122/D, 70126 Bari, Italy; marianna.ambrico@istp.cnr.it (M.A.); giorgio.dilecce@istp.cnr.it (G.D.)

² National Research Council of Italy (CNR), Institute for Sustainable Plant Protection (IPSP), Via Amendola 122/D, 70126 Bari, Italy; stefania.zicca@ipsp.cnr.it (S.Z.); angelo.destradis@cnr.it (A.D.S.); maria.saponari@ipsp.cnr.it (M.S.); donato.boscia@ipsp.cnr.it (D.B.)

³ Department of Soil, Plant and Food Sciences, University of Bari ALDO MORO, Via G. Amendola 165/A, 70126 Bari, Italy; palma.rotondo@uniba.it

* Correspondence: paolofrancesco.ambrico@cnr.it (P.F.A.); pasquale.saldarelli@ipsp.cnr.it (P.S.)

Abstract: The quarantine bacterium *Xylella fastidiosa* was first detected in Salento (Apulia, Italy) in 2013 and caused severe symptoms in olives, leading to plant death. The disease, named Olive Quick Decline Syndrome (OQDS), is caused by the strain “De Donno” ST53 of the subspecies *pauca* of this bacterium (XfDD), which is spread by the insect *Philaenus spumarius*. The epidemic poses a serious threat to the agricultural economy and the landscape, as *X. fastidiosa* infects several plant species and there is yet no recognized solution. Research on OQDS is focused on finding strategies to control its spread or mitigate its symptoms. As a perspective solution, we investigated the efficacy of the low-temperature plasma and plasma-activated water to kill bacterial cells. Experiments were conducted in vitro to test the biocidal effect of the direct application of a Surface Dielectric Barrier Discharge (SDBD) plasma on bacteria cells and Plasma Activated Water (PAW). PAW activity was tested as a possible biocidal agent that can move freely in the xylem network paving the way to test the strategy on infected plants. The results showed a high decontamination rate even for cells of XfDD embedded in biofilms grown on solid media and complete inactivation in liquid culture medium.

Keywords: plasma agriculture; low-temperature plasma; surface dielectric barrier discharges; *Xylella fastidiosa*; plasma activated water



Citation: Ambrico, P.F.; Zicca, S.; Ambrico, M.; Rotondo, P.R.; De Stradis, A.; Dilecce, G.; Saponari, M.; Boscia, D.; Saldarelli, P. Low Temperature Plasma Strategies for *Xylella fastidiosa* Inactivation. *Appl. Sci.* **2022**, *12*, 4711. <https://doi.org/10.3390/app12094711>

Academic Editor: Andrea Sevcovicova

Received: 4 April 2022

Accepted: 4 May 2022

Published: 7 May 2022

Publisher's Note: MDPI stays neutral with regard to jurisdictional claims in published maps and institutional affiliations.



Copyright: © 2022 by the authors. Licensee MDPI, Basel, Switzerland. This article is an open access article distributed under the terms and conditions of the Creative Commons Attribution (CC BY) license (<https://creativecommons.org/licenses/by/4.0/>).

1. Introduction

Xylella fastidiosa (*X. fastidiosa*) is a xylem-limited gammaproteobacterium whose pathogenic mechanism relies on the occlusion of the xylem vessels. The bacterium lives in biofilm communities embedded in an exopolysaccharide matrix from which clumps of cells are released to systemically colonize the infected plants. Infections of new plants are mediated by insect vectors which feed in the xylem, acquire the bacterium, and transmit it to new plants during successive feeding activities [1,2].

The “De Donno” strain of *X. fastidiosa* subspecies *pauca* haplotype ST53 was discovered in late 2013 in the Salento Peninsula (Apulia region) in olive trees showing leaf scorching, extensive branch desiccations, and plant death [3]. Soon after, this bacterial strain was demonstrated to be the causal agent of these symptoms which were reconciled under the name of Olive Quick Decline Syndrome (OQDS) [3]. While affecting the two major autochthonous olive cultivars Ogliarola salentina and Cellina di Nardò, this strain has been found infecting 595 plant species and in several cases without showing symptoms [4].

The finding of *X. fastidiosa* in this new environment and infecting primarily olive stimulated several research programs which led to the description of the epidemiology of the infections in the epidemic area in the Salento Peninsula, the identification of *Philaenus*

spumarius as the insect vector, the genomic of the bacterium and the olive response to the infections [5].

The *X. fastidiosa* epidemic in southern Italy is slowly expanding north to the southern portion of Apulia. However, besides Italy, where a subspecies *multiplex* strain of *X. fastidiosa* was found in Tuscany [6], other strains were discovered in France [7], Spain [8,9], Portugal [10] and recently in Israel [11], which highlights the severe threat that this quarantine bacterium poses to the Mediterranean agriculture.

Generally, bacterial cells are inactivated by physical processes, such as heat and gamma radiation, and chemical processes, such as ethylene oxide, that are not suitable for curing *Xylella*-infected plants. Heat can cause irreversible damage to the plant; ethylene oxide is highly inflammable and toxic, and radiation processes require isolated sites and the safety of operating personnel and can induce DNA damage. Such disadvantages drive research for a novel, highly efficient sterilization process.

Among the microbial inactivation strategies, non-thermal atmospheric pressure plasma has achieved increased attention in biology, medicine [12–14] and the agri-food industry [15–17]. Low-Temperature Plasma (LTP) has potential advantages over conventional methods, such as its controllable level of toxicity, low process operational costs, short treatment time at almost room temperatures and applicability to a wide variety of goods [16,18–21]. Nevertheless, it must be pointed out that plasma characteristics need to be properly defined and a careful selection of device design and system operating parameters are needed to obtain a positive effect on the treated samples [22–24].

Atmospheric air LTP is an excellent source of several antimicrobial agents in the gas phase. [25]. The reactive species produced include electronically and vibrationally excited oxygen O₂ and nitrogen N₂; reactive oxygen species (ROS), such as atomic oxygen O, singlet oxygen ¹O₂, superoxide anion O₂⁻ and ozone O₃ and, if humidity is present, H₂O⁺, OH⁻ anion, OH radical or H₂O₂ [26]; and reactive nitrogen species (RNS), such as atomic nitrogen N, nitrogen metastable state N₂(A) and nitric oxide NO. Target organisms are either directly exposed to the plasma-produced ROS and RNS together with UV light and/or pulsed electric field produced by the plasma. In general ROS species triggers an oxidative stress response leading to detrimental oxidative cell damage [27,28] and the inactivation of microorganisms [29–39]. Hydroxyl radicals (OH) have a direct impact on the cell membranes of microorganisms [40,41].

Besides direct decontamination processes, plasma can also activate stress signalling cascades enabling the self-defence mechanism, particularly in plants. RONS produced in response to abiotic and biotic stresses act as signalling molecules [42], leading to the activation of defence genes [43–48] and the production of defence compounds [49,50]. Moreover, ROS can also make the plant readily available in a redox state to respond quickly to stress [51].

In recent years plasma-activated water (PAW) has attracted the attention of researchers as a possible activated media to be used in decontamination processes [52]. Many studies on PAW indicated that the main active substances of PAW are reactive oxygen species (ROS) and reactive nitrogen species (RNS) [53,54]. The main components of ROS include hydroxyl radicals, hydrogen peroxide, singlet oxygen, superoxide anions, and ozone, whereas RNS mainly includes nitrate, nitrite, peroxyxynitrite, nitric oxide radical, ammonia and nitrogen [55]. Among them, the long-lived reactive species are hydrogen peroxide, nitrate and nitrite. The physical and chemical properties of water, such as conductivity, pH and redox potential are affected by plasma activation.

The research paper on PAW as a control strategy for diseases and insect pests is sporadic and experimental. Two fields of research are followed: one regarding the direct decontamination by PAW and the other the activation of self-defence in the plant. PAW was found to reduce surface yeast [56] and inhibit the mycelium growth of *Fusarium graminearum* [57], to protect tomato plants against leaf spot disease caused by *Xanthomonas vesicatoria* [58]. Irrigation of seedlings and seeds with PAW resulted in better growth

morphology, oxidation and defence gene expression [12,59,60]. In terms of pest control [22], PAW was found effective against *Planococcus citri* [61] revealing a high mortality rate in lab conditions. The mechanism leading to the killing of pathogenic bacteria on the plants' surface [62] can be related to RNS and ROS, which can enter bacterial cells through the immediate pores in the active transport cell membrane. The RNS and ROS can oxidize DNA, proteins and lipids in the cell, breaking DNA, degrading proteins and inducing lipid peroxidation thereby causing the contents to flow out of the bacteria and die [62], with ozone and peroxyxynitrite being the dominant species in the sterilization process [55,63–66]. Many researchers also speculate that acidity and active compounds are related to PAW. In an acidic environment, the RNS and ROS react with the lipids and carbohydrates of the DNA proteins in the cells, lowering the pH of the cells and causing physiological dysfunction and cell death [66]. In addition, the effects of PAW on biofilms have also been explored [67–70]. The importance of biochemically reactive species formed in PAW for the destruction and degradation of the biofilm matrix and the release of resident microbial cells have been highlighted [71]. Moreover, as for Plasma, the PAW can serve as a resistance inducer for plants, triggering their defences against pests and diseases, strengthening the plant pathogen defence pathway through ROS mediated channels [72,73].

In the present manuscript, LTP and PAW were used to evaluate their anti-microbial activities against the “De Donno” strain of *Xylella fastidiosa* subspecies *pauca* haplotype ST53 (XfDD). Due to the difficulties in experimenting in a not confined laboratory, our approach was to create a portable device to produce plasma through a Surface Dielectric Barrier Discharge (SDBD), using ambient air, with a measured relative humidity of about 40%. All the treatments were carried out in a laminar flow hood. We first explore the feasibility of direct plasma decontamination of bacteria by exposing the cellular culture to the spatial afterglow of the SDBD for in vitro culture. The second step consisted in evaluating the effect of PAW in XfDD suspension in a water-based solution. The rationale of the proposed experiments is to find a possible strategy to reach the decontamination of the surfaces exposed to the bacterial, such as tools or leaves, by the application of an atmospheric pressure plasma source, and to apply the PAW as a novel tool to control the infection in plants either by direct exposure of the pathogen to the RONS present in the PAW or by activating the plant self-defence mechanism.

2. Materials and Methods

2.1. Dielectric Barrier Discharge

The discharge system includes an SDBD reactor, gas feeding unit, discharge energization system, electrical and optical diagnostics, and sample holder suitable for inserting biological samples at a selected distance from the discharge surface. The SDBD reactor shown in panel (A) of Figure 1, consists of a planar SDBD electrode system placed in a PVC chamber equipped with gas feed input/output ports and a high voltage (HV) interface.

The discharge was built starting from a glass petri dish, in which the electrodes were included (Figure 1). The ground electrode was equipped with an aluminium air-cooled dissipator to keep its temperature as close as possible to room temperature. The nickel electrode exposed to the discharge consists of 22 parallel stripes (0.2 mm wide, 10 mm long and separated by 1 mm). An aluminium induction electrode (55 mm × 55 mm) covers the opposite surface of the glass petri dish cover plate. The SDBD was powered by an AC power supply based on an Information Unlimited PVM500—Plasma Power Generator. Applied AC HV waveform (19.6 kHz) was amplitude-modulated by a square-wave modulation waveform ($f_M = 500$ Hz) producing 19.6 kHz sine-wave T_{ON} and T_{OFF} periods with a fixed duty cycle $D = T_{ON} / (T_{ON} + T_{OFF}) = 25\%$ and a precise number of sine-wave bursts were selected through an external trigger realized using a TG 5011 Function Generator (TTi). We used Keysight InfiniiVision MSOX6004A Mixed-signal oscilloscope (bandwidth 1 GHz, up to 20 GS/s) to record the voltage–charge, voltage–current characteristics of the discharge. We used a Tektronix P6015A high voltage probe (1000:1@1 M Ω , bandwidth 75 MHz) to monitor voltage waveforms, a Magnelab current transformer model CT-C1.0 (bandwidth

200 Hz–500 MHz) to measure the plasma current, and a voltage probe (100:1@10 MW, bandwidth 1 GHz) to measure the potential drop on a transferred charge measuring capacitor ($C = 2.5$ nF) inserted between the induction electrode and ground. The reactor was fed with humid air at a fixed flow rate of 7 slm. This reactor chamber allows the insertion of 50 mm in diameter standard Petri dishes (Figure 1) next to the SDBD surface, with the top border approximately 3 mm far from the HV electrode. The same discharge setup was used to produce plasma-activated water (PAW).

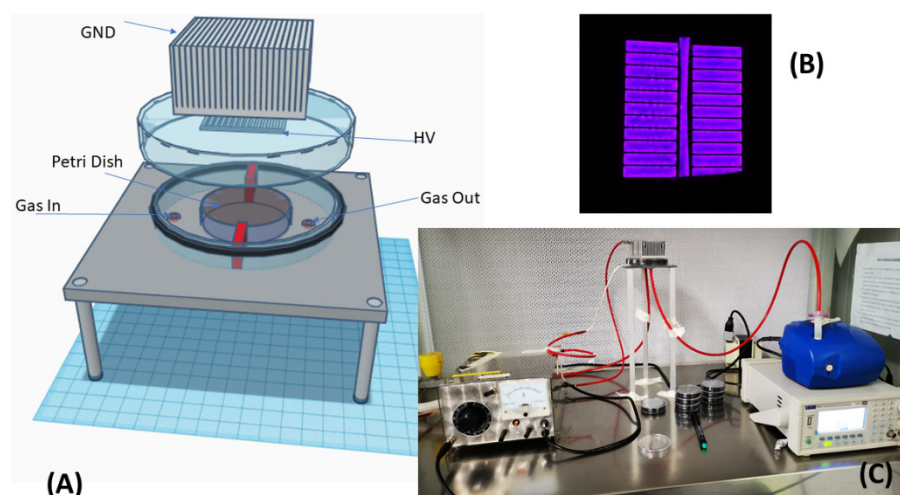


Figure 1. Experimental setup: (A) SDBD discharge reactor; (B) plasma produced on SDBD Surface in the air; (C) setup under a laminar flow hood.

The typical appearance of the HV electrode during the on-time is shown in Figure 1 B. Since we are dealing with quarantine bacteria the discharge was operated under a laminar flow hood (model Aura HZ48), in the authorized lab of the CNR IPSP in Bari (Figure 1C).

2.2. Emission Spectroscopy

To perform the spectroscopic measurement, a slightly modified version of the reactor was used to place UV grade quartz frontal windows allowing direct visual control of the discharge area and optical emission diagnostics. Optical emission spectroscopy was performed by collecting light from the SDBD plasma surface through a UV fused silica single-lens fibre optic bundle model LG-455-020-3 (3 m, 190 to 1100 nm, with 19 fibres ($\phi = 200$ μm), 10 mm ferrule at slit end) equipped with UV grade quartz lenses system on the entrance slit of a monochromator. The imaged area collected light is limited by the entrance slit dimension and can reach a maximum size of 3 (l) \times 5 (h) mm^2 . The light is spectrally resolved by a 30 cm spectrometer (Acton Spectra Pro 2300), equipped with a multiple-grating turret with a 300/600/1200 grooves mm^{-1} , blazed at 300 nm and covering the ranges 200–1400 nm. The spectrum is acquired with a Princeton Instruments PI-MAX4 1024i ICCD camera equipped with a 1024 \times 1024 pixel sensor (size 12.8 μm , active area 13.1 \times 13.1 mm^2). One CCD image of a spectrum covers a range of approximately 144/65/30 nm, respectively, for the three different gratings. The intensities of the emission spectra acquired by the ICCD detector were spectral, and intensities were corrected utilizing Halogen (oriel) and calibration lamps (oriel). The spectra were used to evaluate rotational temperatures and nitrogen vibrational distributions. Spectra were simulated to infer rotational temperature information using the freely available spectroscopic tool Massive OES [74–76].

2.3. PAW Characterization

An aliquot of 3 mL of ultrapure water was treated at different times (5, 15 and 30 min) with Surface Dielectric Barrier Discharge plasma (SDBD) to evaluate the change in the

content of nitrates and nitrites, H_2O_2 and pH value and the changes in the electric properties. The treatment times were progressively increased to study changes in the water compared with the untreated sample. Three replicates of measurement were set up and the mean value was recorded. The pH value was measured with the pH meter pH50 Lab (XS Instruments, Carpi, MO, Italy) at room temperature.

The content in nitrates and nitrites was measured with a UV-Visible Spectrophotometer Thermo Scientific™ Evolution™ 201 (Thermo Fisher Scientific Inc., Madison, WI, USA) following the protocol indicated in the Nitrate and Nitrite Test Spectroquant® (Merck KGaA, Darmstadt, Germany). The Nitrite content was evaluated at the absorbance value of 525 nm with the dilution of 1:5 of the water sample, following the kit procedure parameters, whereas the nitrate content was evaluated at 340 nm without dilution of the water sample. The peroxide (H_2O_2) content in the analysed water was measured with the Peroxide Test MQuant® (Merck KGaA).

Measures were repeated 24 h after the activation of water, in samples treated and kept at 4 °C, to evaluate changes in the content during the time.

2.4. *Xylella fastidiosa* Growth Conditions and Plasma Treatments

X. fastidiosa subsp. *pauca* strain “De Donno” ST53 was used in this study [77]. Bacteria were cultured on BCYE agar plates for 15–20 days at 28 °C. Plasma treatments were carried out on bacteria that directly grow on solid (agar amended) media or after suspension in PAW.

2.4.1. Treatment of Agar Surface-Grown Bacteria

XfDD was currently grown on BCYE agar plates at 28 °C and the inoculum was regularly renewed every 7 days on new plates. Cells were collected from the agar surface with a sterile loop, resuspended in $1 \times$ PBS buffer and adjusted, before plating, to a final concentration of 4×10^8 CFU mL⁻¹ (OD600 0.5).

Trials were carried out using different bacteria concentrations, from 10^7 to 10^3 CFU mL⁻¹ after resuspending cells scraped from an agar plate in PBS. Forty microliters of bacteria were plated by spreading on the agar surface using a sterile loop. Preliminary tests were carried out to find the best conditions of treatments, particularly referring to the initial bacteria concentration, the pre-culture of the bacteria before plasma exposure and the duration of the exposure. To this aim, bacteria were pre-cultured for 1 and 5 days before being exposed to LTP which was discharged for 10, 100 and 200 s. LTP untreated cells grown in the same conditions were used as control. The plates were incubated at 28 °C for up to 30 days, and the antibacterial activity was assessed using the viable plate count method [78]. The number of CFU mL⁻¹ in the control plate was determined by multiplying the number of colonies on a dilution plate by the corresponding dilution factor. Only plates (or replicate plates from the same dilution) with 30–300 colonies were counted [79].

In addition, the cumulative effect of the LTP was evaluated by applying the SDBD plasma (a) one time a day for 1 week, and (b) one time a week for 3 weeks at the maximum exposure time of 200 s. In these trials, XfDD was pre-cultured for 1 and 7 days in (a) and (b) respectively, before being exposed to LTP treatment.

Plates were preliminarily treated with LTP for an exposure time of 200 s and successively inoculated with XfDD to evaluate if the plasma treatment could alter the chemical/physical properties of the BCYE agar substrate and therefore inhibit the growth of the bacterium. Each assay was performed in triplicate, and each experiment was repeated at least twice.

2.4.2. Treatment Cells with Plasma Activated Water (PAW)

Deionized water (DIW) (18.2 MΩ·cm at STP) was obtained from a Millipore Direct-Q 3UV system. A volume of 500 mL of DIW were stored in a container in an ambient atmosphere for one day. This procedure enabled the concentrations of gases dissolved within the DIW to equilibrate with the air, which ensured constant concentrations of gases

between experiments. Three mL of DIW were transferred to a 50 mm-diameter petri dish inserted in the SDBD discharge chamber and treated for 15 min. The free surface of the water was approximately 3 mm far from the SDBD HV electrode. The PAW was then immediately used to resuspend bacteria to a final concentration of 10^7 CFU mL⁻¹. The LIVE/DEAD® BacLight™ (Molecular Probes) viability kit was used to assess the viability of bacteria cells treated with PAW. The kit contains a vial of microsphere suspension and two nucleic acid dyes SYTO 9 and propidium iodide (PI) that allow distinguishing live cells with intact plasma membranes (green) from dead bacteria with compromised membranes (red). Bacteria suspensions were incubated at room temperature for 15 min in the dark in a solution of equal volumes of the two stains. Photomicrographs were taken on a Nikon E800 microscope using a fluorescein isothiocyanate (480/30 excitation filter, DM505 dichroic mirror, 535/40 emission filter) and tetramethylrhodamine isocyanate (546/10 excitation filter, DM575 dichroic mirror, 590 emission filter) fluorescence filter sets.

3. Results

3.1. Plasma Current Voltage and Emission Spectroscopy

The SDBD was operated in humid ambient air (25 °C, 40% RH) at atmospheric pressure. The applied AC voltage (20.6 kVpp (peak-to-peak); see Figure 2) consisted of repetitive bursts (repetition rate 500Hz), each consisting of nine AC cycles (fAC = 19.6 kHz) with a repetition rate of 500 Hz (duty cycle of 0.25). In this way, we obtained a homogeneous distribution of micro-discharges. The actual discharge ON-time is shorter than the duration of the AC cycles. We can estimate an effective duty cycle of the order of 0.1 of the nominal one.

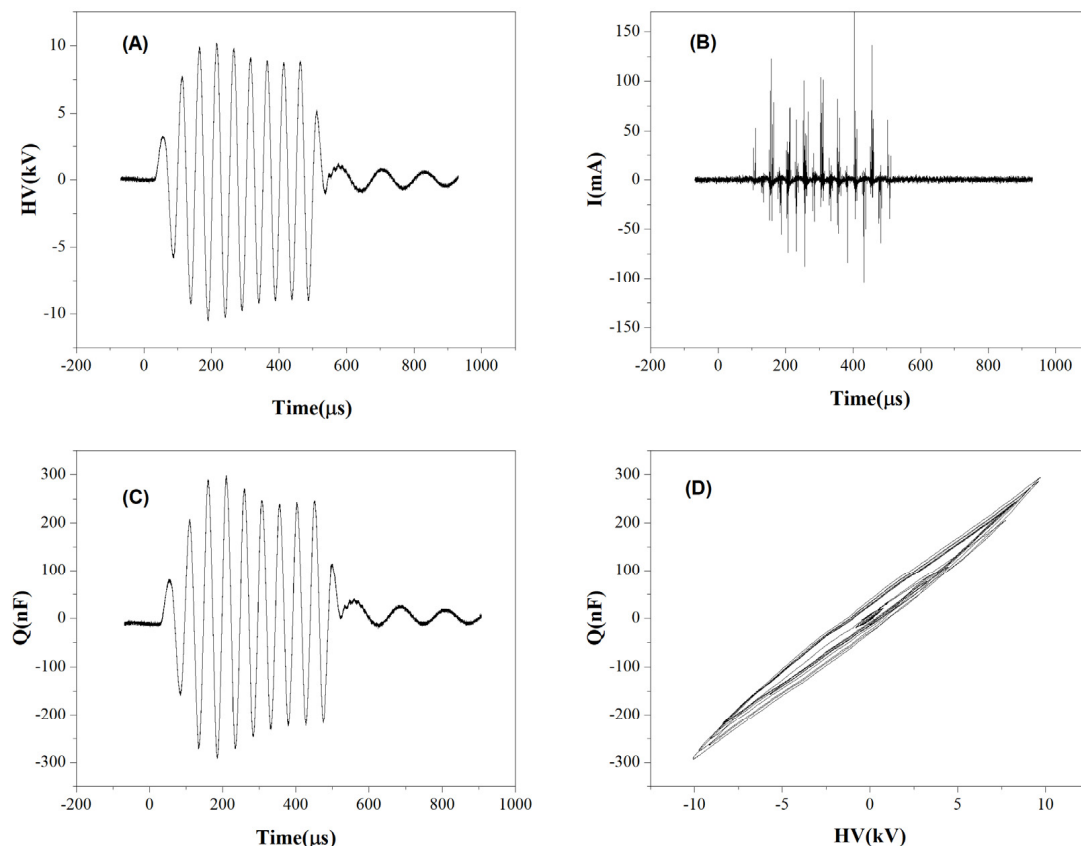


Figure 2. Typical waveform for 1 burst applied to the discharge reactor: (A) voltage; (B) current; (C) charge; (D) Lissajous figure for estimating the burst energy deposited in the plasma phase.

This ensures that biological samples are not exposed to excessively damaging temperatures. Typical voltage, current, and charge characteristics are shown in Figure 2A–C, along

with the typical Lissajous figure showing the charge voltage characteristic (Figure 2D) used to determine the discharge energy. The estimated energy per burst is about 4.5 mJ, i.e., an average power of 2.25 W, with an energy density of $3.8 \cdot 10^{-2} \text{ Wh L}^{-1}$. With this energy density, the air-SDBD is operated in ozone mode, and we can expect a concentration on the order of 200–300 ppm, well above the concentration of nitrogen oxide products [30]. The total power consumption of the plasma device was measured and estimated at 5W with an energy transfer to the plasma of 45%.

Figure 3 shows low-resolution emission spectra of filamentary SDBD operating in humid air and reveals strong bands of the second positive system (SPS) ($C^3\Pi_u \rightarrow B^3\Pi_g$) of N_2 and the first negative system (FNS) ($B^2\Sigma_u^+ \rightarrow X^2\Sigma_g^+$) of N_2^+ in the UV spectral region. In the Vis-NIR region, we observed characteristic sequences of bands of the first positive system (FPS) ($B^3\Pi_g \rightarrow A^3\Sigma_u^+$) of N_2 . The emission line for atomic oxygen was observed at 777 nm, indicating the production of atomic oxygen during the plasma phase.

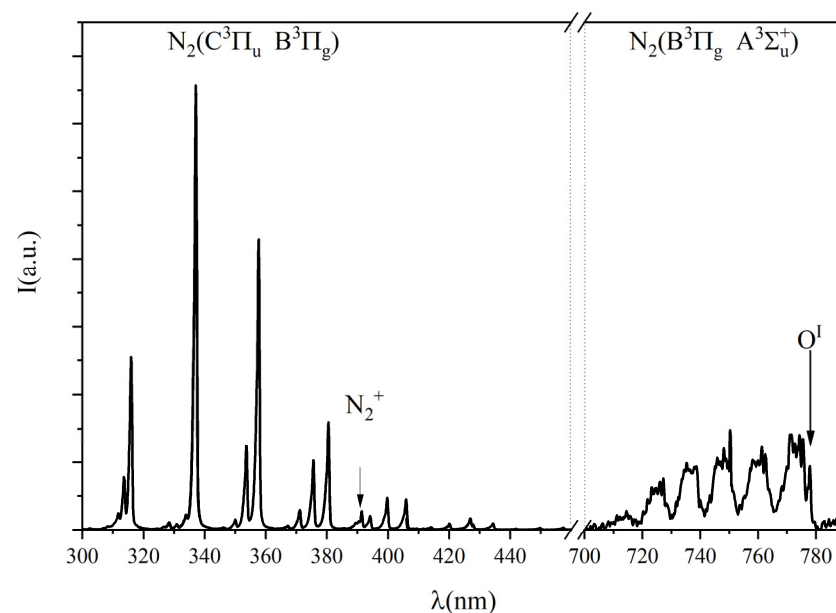


Figure 3. Typical averaged (1000 shots) electron impact induced emission spectrum intensity ($I(\text{a.u.})$) as a function of wavelength ($\lambda(\text{nm})$) over multiple discharge filaments developing over the entire ON time AC HV burst.

A detailed analysis of the emission spectra allows the measurement of the gas temperature and the local reduced electric field, E/N , i.e., the electric field divided by the concentration of gas molecules. Moreover, a reasonable estimation of the nitrogen vibrational temperature (T_v) is possible. There is no room here to explain the complex analysis procedure that can be found in [80,81]. It is important here to point out that this analysis is based on the fact that the observed emissions originated from electronic states that are populated by electron impact. In other words, these emissions come from the active discharge sites, i.e., the micro-discharges, and therefore, the quantities inferred are “average” values within the micro-discharges. In this way, they are representative of the conditions that initiate the plasma chemistry by excitation and dissociations induced by electron impact.

The gas temperature, in such conditions, is equal to the rotational temperature of the emitting molecules. The partially resolved structures of SPS (0,0) shown in Figure 4 were analysed using the Massive OES spectroscopy tool [74–76]. The SPS (0,0) band can be fitted for a specific instrumental function by setting the rotational temperature to $350 \pm 25 \text{ K}$.

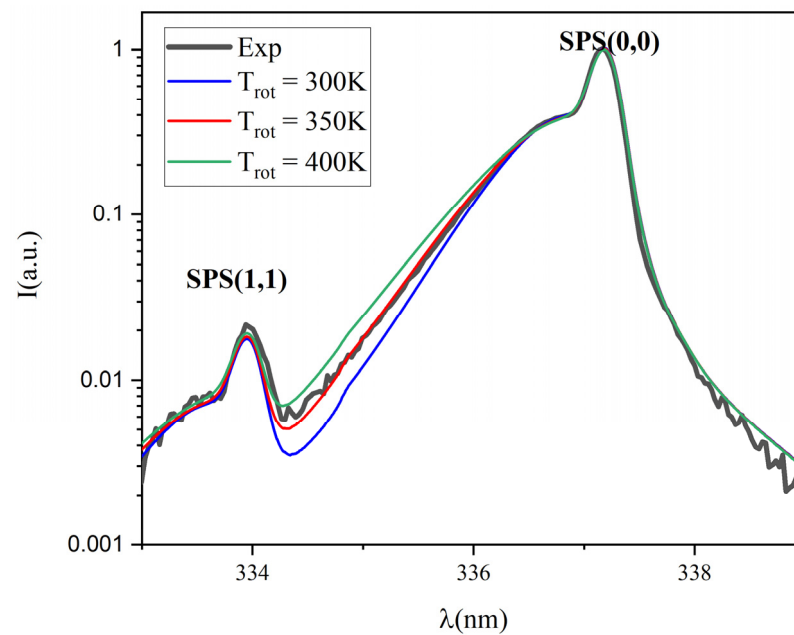


Figure 4. SPS (0,0) band emission (solid line) and simulated band profile for three different temperatures.

This temperature represents the gas temperature, during the discharge on phase, of the plasma that is confined just a few hundred micrometres above the dielectric surface. Thus, it does not represent the actual temperature of the gas in direct contact with the treated substrate. Moreover, considering that the gas flows at 7 slm, a residence time in the discharge volume of 64 ms is sufficiently small to rule out heat accumulation within the gap. This is also evidenced by the temperature of the ground electrodes and the substrate just after the plasma treatment which is close to room temperature.

Figure 4 shows the experimental SPS (0,0) band profile along with three synthetic profiles (simulated for rotational temperatures of 300, 350 and 400 K) on a logarithmic scale to demonstrate the sensitivity of the band tail of the band (formed by the overlap of the R_1 , R_2 and R_3 branches) to the rotational temperature of the $C^3\Pi_u$ state.

Figure 5 shows the emission formed by the $\Delta v = -3$ and -2 sequences of the SPS and by the $\Delta v = 0$ sequences of the FNS. From the ratio between FNS and SPS bands, it is possible to infer the average reduced electric field (E/N) value. A value of (1140 ± 60) Td is deduced ($1 \text{ Td} = 10^{-17} \text{ V cm}^2$) corresponding to an electric field value of about $2.35 \times 10^5 \text{ V cm}^{-1}$. This is a pretty high value. It must be understood that micro-discharges evolve according to local electric fields, due to the accumulation of space charge on the streamer's head. Local electric field values can then be much larger than the simply applied voltage divided by the inter-electrodes gap. High local E/N is typical of surface discharges, where the micro-discharges spread over the surface with electric fields enhanced by the surface itself and its microscopic roughness. From the relative intensities of the vibrational bands of the SPS system, the vibrational temperature T_v of the N_2 ground state is inferred to be about 1300 K. This is quite a low value, due to the close vicinity of the surface where the vibrational energy of molecules is readily lost. It must be underlined that all these discharge parameters are relevant to the discharge region, which is confined in a thin layer adjacent to the surface, whose thickness is of the order of 100 μm . They have then no direct influence on the cells, which are at least 3 mm apart from the discharge.

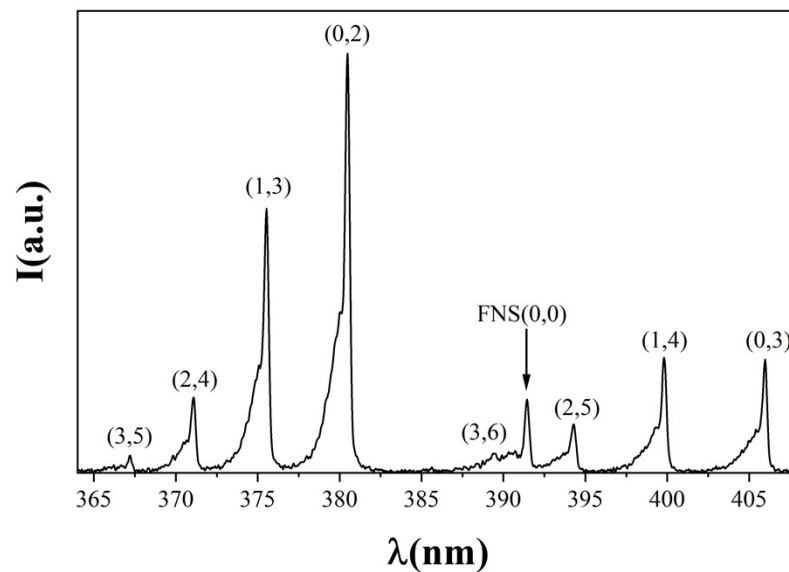


Figure 5. Emission spectra of SPS.

3.2. PAW Characterization

The content of nitrate and nitrite (mg/L) of PAW was measured, and their stability in water after plasma activation was evaluated. The mean value of nitrate (25.7 mg/L) in the water sample exposed to 15 min of SDBD plasma activation was kept almost constant (22.8 mg/L), while the nitrite content was drastically reduced (started from 26.9 mg/L to 16.4 mg/L) after 24 h storage at 4 °C from the activation. The pH value increased from an initial mean value of 3.4 to 4.3. The level of hydrogen peroxide measured through a colorimetric test decreased from 5–10 mg/L to 2–5 mg/L.

3.3. XfDD Growth Conditions and Plasma Treatments

Treatment of Agar Surface-Grown Bacteria

Preliminary investigations showed that the plasma pre-treatment of the agar plates did not alter the growth of XfDD cells (data not shown).

When bacteria (10^7 CFU mL⁻¹) were plated out on Buffered Charcoal Yeast Extract (BCYE) agar and exposed to SDBD for 200 s, complete inhibition of cell growth was observed, whereas after 100 s and 10 s of exposure (Figure 6) there was less pronounced but time-dependent inhibition.

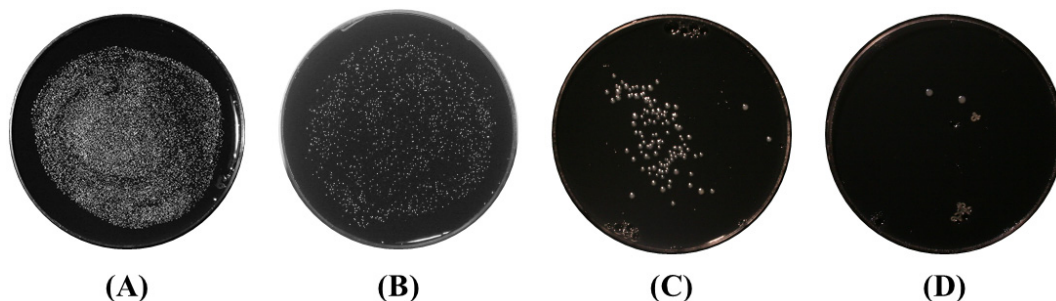


Figure 6. Time-dependent inhibition of XfDD growth by plasma exposure of cells discharged 1 day after plating. Photos were taken after 15 days post-exposure. The figure reports typical results for cells untreated (A) and treated for 10 (B), 100 (C), and 200 (D) s.

Since it is difficult to quantify the effect of plasma treatment by counting colonies at a concentration of 10^7 CFU mL⁻¹ (Figure 7), decimal dilutions from 10^5 to 10^3 CFU mL⁻¹ of XfDD inoculum were applied to the BCYE agar plates in subsequent experiments (trials).

Final SDBD plasma treatment conditions were therefore performed on cells grown 1–5 days after seeding, with a maximum exposure time of 200 s.

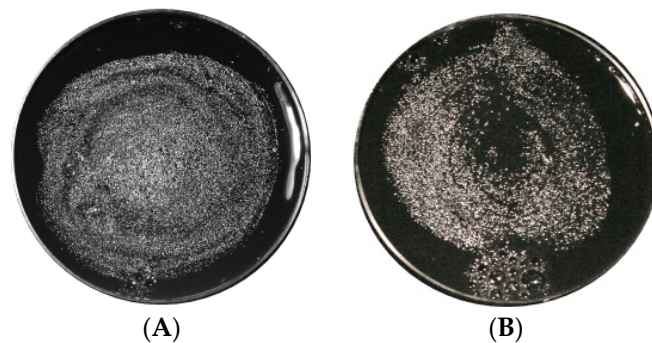


Figure 7. Effect of plasma treatment on XfDD strains (concentration 10^7) grown for 10 days (A) on the substrates before plasma treatment. Pictures were taken 15 days after plasma treatment. The picture shows the growth at 15 days from the plasma treatment of untreated samples (A) versus treated samples (B).

Table 1 shows the results for three different dilutions (10^3 , 10^4 and 10^5) for untreated and 200 s treated plates pre-cultured for one or five days before LTP exposure. The treatment was effective and completely removed all bacteria by plasma, at both 1 and 5 days.

Table 1. Results of the experiment performed on agar surface grown XfDD. Treatment time was fixed at 200 s following the finding of the previous experiment. We performed experiments in triplicate for a total of 9 dishes each experiment. The experiments were conducted on plates just at T0 = 0 and T5 = 5 days after XfDD seeding.

	Time	N of Replicas	11 Days CFU mL ⁻¹	13 Days CFU mL ⁻¹
10^5	untreated	3	$3.81 \times 10^8 \pm 3.7 \times 10^6$	$9.79 \times 10^8 \pm 8.7 \times 10^6$
10^4		3	$4.17 \times 10^5 \pm 2.7 \times 10^5$	$2.17 \times 10^7 \pm 3.8 \times 10^5$
10^3		3	0.00	$1.92 \times 10^5 \pm 3.8 \times 10^4$
10^5	T0	3	0.00	0.00
10^4		3	0.00	0.00
10^3		3	0.00	0.00
10^5	T5	3	0.00	0.00
10^4		3	0.00	0.00
10^3		3	0.00	0.00

When plasma interacts with a surface, its energy (in the form of ions, RONS and UV radiation) is deposited in the exposed matrix. Multiple exposures result in a cumulative effect of absorbed doses leading to progressive destruction of the microorganism. To evaluate the LTP dose–effect, we performed a repetitive plasma treatment of 200 s on plates pre-cultured for seven days before LTP exposure with two different frequencies: 1 treatment per day for a period of 10 days (Trial a, treatment performed in days from 0 to 9) and once per week for a period of three weeks (Trial b, treatment performed in days 0, 7, 15).

The results of these experiments are given in Table 2.

If we compare the log growth of NT samples to treated samples, we can observe that in Trial (a) a strong effect of cumulative dose was observed, with complete removal of bacteria at the lowest initial concentration (10^3 CFU mL⁻¹) and almost a LOG 3 lower growth for higher concentration. In Trial (b), cells were counted just after the last treatment, on day 15, and on day 20 after the first LTP treatment. Treatment resulted on day 20 in lower growth of almost log 4 for the 10^3 concentrations and log3 for the 10^4 , while at 10^5 ,

we cannot exactly estimate the difference in log growth, but colonies for treated samples were countable on the contrary of the untreated one.

Table 2. Results of the dose dependence experiment performed on BYCE agar surface-grown XfDD.

Treatment Frequency	CSUSPENSION (CFU mL ⁻¹)	C11 11 DAYS	LOG GROWTH	C13 13 DAYS	LOG GROWTH	C15 15 DAYS	LOG GROWTH	C20 20 DAYS	LOG GROWTH
NT	10 ⁵	1.1 × 10 ⁹ ± 3.8 × 10 ⁶	9	1.9 × 10 ⁹ ± 8.7 × 10 ⁶	9.3			NC	NC
	10 ⁴	1.2 × 10 ⁶ ± 3.8 × 10 ⁵	6.1	6.5 × 10 ⁷ ± 9.5 × 10 ⁵	7.8			7.5 × 10 ⁸ ± 1.3 × 10 ⁶	8.9
	10 ³	0.0		6.0 × 10 ⁵ ± 8.7 × 10 ⁴	5.8			2.9 × 10 ⁸ ± 6.3 × 10 ⁴	8.5
TRIAL (A) 1/DAY	10 ⁵	3.3 × 10 ⁶ ± 1.4 × 10 ⁶	6.5	4.2 × 10 ⁶ ± 1.4 × 10 ⁶	6.6				
	10 ⁴	1.3 × 10 ⁴ ± 0.7 × 10 ⁴	4.1	1.7 × 10 ⁵ ± 1.4 × 10 ⁵	5.2				
	10 ³	0.0	0	0.0	0.0				
TRIAL (B) 1/WEEK	10 ⁵					3.4 × 10 ⁷ ± 6.3 × 10 ⁶	7.5	1.6 × 10 ⁸ ± 5.2 × 10 ⁶	8.2
	10 ⁴					3.3 × 10 ⁵ ± 1.4 × 10 ⁵	5.5	1.7 × 10 ⁶ ± 1.4 × 10 ⁵	6.2
	10 ³					0.0	0.0	1.0 × 10 ⁵ ± 5 × 10 ⁴	5

3.4. Inactivation of Suspension of *X. fastidiosa* by Plasma Activated Water

It has been shown that the effect of the active species produced in PAW on bacteria depends on the bacterial species. In general, Gram-negative bacteria, such as XfDD, were found to be more sensitive to PAW than Gram-positive bacteria due to significant differences in cell wall structures, physiological state and ultimately planktonic or biofilm status [67]. To test the efficacy of plasma treatment and its potential for use in vivo, bacteria were suspended in PAW previously treated in the SDBD discharge chamber for 15 min. To decipher the exact mode of action of the plasma treatment, its effect on XfDD was monitored using viability assays with fluorescence live/dead staining.

Fluorescent probes were used to assess cell membrane integrity and XfDD viability after incubation in PAW. The untreated control cells were almost all stained green with SYTO 9, indicating that they were viable. A small number of cells were stained red with propidium iodide (PI), indicating that they were probably dead (Figure 8A). The number of cells stained red with PI increased dramatically after treatment with PAW, while cells stained with SYTO 9 decreased as expected, and only a few fluorescent cells were visible after treatment (Figure 8B). This indicates that the integrity of the cell membrane of the bacteria was damaged by the treatment, affecting their viability.

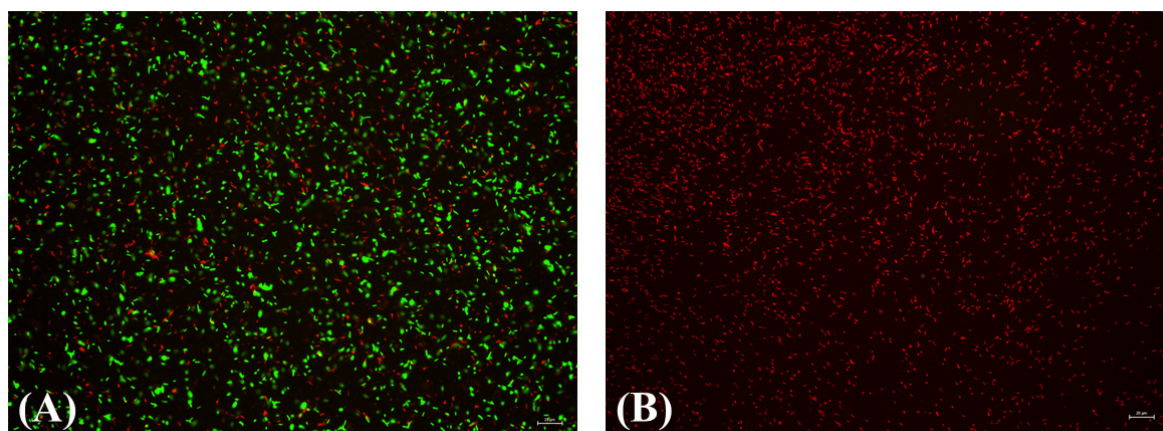


Figure 8. Typical fluorescence images of XfDD suspension in water for the untreated (A), and PAW treated (B) samples.

4. Discussion and Conclusions

In the present study, we investigated the effects of Air LTP application on XfDD inactivation.

Air plasma is a rather complex environment in terms of chemical composition (RONS) and light emission (from UV to mid-range IR, mainly due to molecular nitrogen systems). Using the optical emission spectrum (OES) recorded at about 3 mm from the SBDB surface, we observed weak emissions from the Nitric Oxide gamma-band covering the UV-C region (200–280 nm), from OH (mainly in the presence of water) and N₂ SPS in the UV-B region (280–315 nm). Thus, direct photooxidation of the protein coat is not considered to be the dominant inactivation process. The strongest emission was observed in the UV-A region (315–400 nm), due to the SPS, FNS band systems of N₂. Although we cannot exclude UV-A-mediated bacterial disinfection [82,83], this cannot be the main process leading to cell death due to the reported exposure time and energy density.

From the SPS (0,0) emission and comparison with the corresponding simulation spectra, we can also rule out heat as a possible mechanism for the disinfection of the samples.

From the emission spectroscopy in the mid- IR, we also observed the presence of atomic oxygen at 777 nm. Moreover, due to the energy density used, we can also deduce that the discharge is operating in ozone mode since ozone is the main post-discharge product along with a small part of NO_x present as post-discharge products. Thus, the main disinfection mechanism could be due to oxidative pressure by the reactive oxygen and nitrogen species (RONS), which are produced by plasma and are toxic to bacterial pathogens at high concentrations. These RONS oxidize proteins, lipids and nucleic acids and lead to the destruction of the pathogen or abrogate bacterial pathogenicity [84].

The efficacy of the treatment fixed at 200 s makes disinfection a rather rapid process in the case of planktonic cells. Moreover, pre-treatment of the cell culture medium with plasma does not result in sufficient changes in substrate chemistry leading to apoptosis of the cells. The presence of biofilm in the cell culture makes it more difficult to treat with only one discharge run at the selected treatment time. This can be overcome by increasing the plasma dose. Since we wanted to keep the plasma parameters constant, we decided to increase the plasma dose by repeating the treatment with a different frequency. This guarantees that we keep the temperature of the plasma phase close to room temperature and preserve the electrode from possible failure.

In this case, the best results were obtained with a repeated daily treatment for 1 week, which stopped cell growth and resulted in at least a log-2 lower growth in bacterial colonies to untreated samples.

For the practical use of LTP, the bacteria must be treated in their natural habitat, the xylem vessels of the plant. To meet these biological requirements, we investigated the inactivation properties of PAW in liquid culture. The nontoxic effect of PAW on plants has been tested in side experiments on tomato plants (results not shown) and also reported in recent literature making this approach a possible active medium to control XfDD in plants [85,86].

In our experiment, we used freshly prepared PAW obtained by activation of sterile water by SBDB in air. Assuming that the activity of PAW in terms of sterilization properties is due to the presence of peroxy-nitrous acid (which requires nitrite, peroxide and acidic conditions) [53], freshly prepared PAW by cold plasma processes should be the most efficient means. Chemical analysis of freshly prepared PAW at a treatment time of 15 min showed the presence of nitrite, nitrate and hydrogen peroxide. The high nitrate, nitrite and peroxide content of the freshly produced PAW was indicative of the best treatment efficacy in this case. Nevertheless, the PAW proved to be sufficiently stable for 1 day when stored in an opaque container at a temperature of 4 °C.

Our results showed that PAW has excellent antimicrobial potential to inactivate *X. fastidiosa* cells. Just 15 min of treatment is sufficient to destroy XfDD cells in liquid culture in vitro experiments. This is an important step towards the development of plasma-assisted strategies to inhibit the growth or kill XfDD in the xylem vessels of plants and to apply an

environmentally safe strategy to control this pathogen, which is the current focus of our research activities.

Author Contributions: P.F.A. designed and conducted the experiments and wrote the manuscript; S.Z. conducted the experiment(s) and wrote part of the manuscript; M.A. conducted the experiment(s) and wrote part of the manuscript; P.R.R. conducted the experiment(s) and wrote part of the manuscript; G.D. performed spectroscopic analysis and critically revised it; M.S. carried out critical revision and manuscript writing; D.B. carried out critical revision and manuscript writing; A.D.S. carried out lab work and manuscript writing; P.S. carried out experimental plan, critical revision and manuscript writing. All authors have read and agreed to the published version of the manuscript.

Funding: This work was partially funded by Italian Ministero dello Sviluppo Economico [Project PROTECTION; Programma Operativo Nazionale «Imprese e Competitività» 2014–2020 FESR; grant number Protection F/050421/01-03/X32]. P.F.A. and M.A. acknowledge the Potenziamento Strutturale PONa3_00369 “Laboratorio per lo Sviluppo Integrato delle Scienze e delle TECnologie dei Materiali Avanzati e per dispositivi innovativi (SISTEMA)” dell’Università degli Studi di Bari “A. Moro”.

Institutional Review Board Statement: Not applicable.

Informed Consent Statement: Not applicable.

Conflicts of Interest: The authors declare no conflict of interest.

References

- Redak, R.A.; Purcell, A.H.; Lopes, J.R.S.; Blua, M.J.; Mizell, R.F.; Andersen, P.C. The Biology of Xylem Fluid-Feeding Insect Vectors of *Xylella fastidiosa* and Their Relation to Disease Epidemiology. *Annu. Rev. Entomol.* **2004**, *49*, 243–270. [CrossRef] [PubMed]
- Schaad, N.W.; Postnikova, E.; Lacy, G.; Fatmi, M.; Chang, C.-J. *Xylella fastidiosa* Subspecies: *X. fastidiosa* Subsp. Piercei, Subsp. Nov., *X. fastidiosa* Subsp. Multiplex Subsp. Nov., and *X. fastidiosa* Subsp. Pauca Subsp. Nov. *Syst. Appl. Microbiol.* **2004**, *27*, 290–300. [CrossRef] [PubMed]
- Saponari, M.; Giampetruzzi, A.; Loconsole, G.; Boscia, D.; Saldarelli, P. *Xylella fastidiosa* in Olive in Apulia: Where We Stand. *Phytopathology* **2019**, *109*, 175–186. [CrossRef] [PubMed]
- European Food Safety Authority (EFSA). Update of the *Xylella* spp. Host Plant Database—Systematic Literature Search up to 30 June 2019. *EFSA J.* **2020**, *18*, e06114. [CrossRef]
- Saponari, M.; Boscia, D.; Altamura, G.; Loconsole, G.; Zicca, S.; D’Attoma, G.; Morelli, M.; Palmisano, F.; Saponari, A.; Tavano, D.; et al. Isolation and Pathogenicity of *Xylella fastidiosa* Associated to the Olive Quick Decline Syndrome in Southern Italy. *Sci. Rep.* **2017**, *7*, 17723. [CrossRef]
- Marchi, G.; Rizzo, D.; Ranaldi, F.; Ghelardini, L.; Ricciolini, M.; Scarpelli, I.; Drosera, L.; Goti, E.; Capretti, P.; Surico, G. First Detection of *Xylella fastidiosa* Subsp. Multiplex DNA in Tuscany (Italy). *Phytopathol. Mediterr.* **2018**, *57*, 363–364.
- Soubeyrand, S.; de Jerphanion, P.; Martin, O.; Saussac, M.; Manceau, C.; Hendrikx, P.; Lannou, C. Inferring Pathogen Dynamics from Temporal Count Data: The Emergence of *Xylella fastidiosa* in France Is Probably Not Recent. *New Phytol.* **2018**, *219*, 824–836. [CrossRef]
- Olmo, D.; Nieto, A.; Borràs, D.; Montesinos, M.; Adrover, F.; Pascual, A.; Gost, P.A.; Quetglas, B.; Urbano, A.; de Dios García, J.; et al. Landscape Epidemiology of *Xylella fastidiosa* in the Balearic Islands. *Agronomy* **2021**, *11*, 473. [CrossRef]
- Xylella fastidiosa*. Available online: <https://www.mapa.gob.es/es/agricultura/temas/sanidad-vegetal/organismos-nocivos/xylella-fastidiosa/> (accessed on 1 April 2022).
- Delbianco, A.; Gibin, D.; Pasinato, L.; Morelli, M. Update of the *Xylella* spp. Host Plant Database—Systematic Literature Search up to 31 December 2020. *EFSA J.* **2021**, *19*, e06674. [CrossRef]
- First Report of *Xylella fastidiosa* in Israel 2019/121. Available online: <https://gd.eppo.int/reporting/article-6551> (accessed on 1 April 2022).
- Kaushik, N.K.; Ghimire, B.; Li, Y.; Adhikari, M.; Veerana, M.; Kaushik, N.; Jha, N.; Adhikari, B.; Lee, S.-J.; Masur, K.; et al. Biological and Medical Applications of Plasma-Activated Media, Water and Solutions. *Biol. Chem.* **2018**, *400*, 39–62. [CrossRef]
- Martines, E. Special Issue “Plasma Technology for Biomedical Applications”. *Appl. Sci.* **2020**, *10*, 1524. [CrossRef]
- Choi, E.H.; Uhm, H.S.; Kaushik, N.K. Plasma Bioscience and Its Application to Medicine. *AAPPS Bull.* **2021**, *31*, 1–38. [CrossRef]
- Puač, N.; Gherardi, M.; Shiratani, M. Plasma Agriculture: A Rapidly Emerging Field. *Plasma Process. Polym.* **2018**, *15*, 1700174. [CrossRef]
- Ambrico, P.F.; Šimek, M.; Rotolo, C.; Morano, M.; Minafra, A.; Ambrico, M.; Pollastro, S.; Gerin, D.; Faretra, F.; De Miccolis Angelini, R.M. Surface Dielectric Barrier Discharge Plasma: A Suitable Measure against Fungal Plant Pathogens. *Sci. Rep.* **2020**, *10*, 1–17. [CrossRef] [PubMed]
- Misra, N.N.; Tiwari, B.K.; Raghavarao, K.S.M.S.; Cullen, P.J. Nonthermal Plasma Inactivation of Food-Borne Pathogens. *Food Eng. Rev.* **2011**, *3*, 159–170. [CrossRef]

18. Hähnel, M.; Von Woedtke, T.; Weltmann, K.D. Influence of the Air Humidity on the Reduction of Bacillus Spores in a Defined Environment at Atmospheric Pressure Using a Dielectric Barrier Surface Discharge. *Plasma Process. Polym.* **2010**, *7*, 244–249. [[CrossRef](#)]
19. Ambrico, P.F.; Šimek, M.; Morano, M.; De Miccolis Angelini, R.M.; Minafra, A.; Trotti, P.; Ambrico, M.; Prukner, V.; Faretra, F. Reduction of Microbial Contamination and Improvement of Germination of Sweet Basil (*Ocimum basilicum* L.) Seeds via Surface Dielectric Barrier Discharge. *J. Phys. D. Appl. Phys.* **2017**, *50*, 305401. [[CrossRef](#)]
20. Guo, J.; Huang, K.; Wang, J. Bactericidal Effect of Various Non-Thermal Plasma Agents and the Influence of Experimental Conditions in Microbial Inactivation: A Review. *Food Control* **2015**, *50*, 482–490. [[CrossRef](#)]
21. Keener, K.M.M.; Misra, N.N.N. *Future of Cold Plasma in Food Processing*; Elsevier Inc.: Amsterdam, The Netherlands, 2016; ISBN 9780128013656.
22. Dobrynin, D.; Fridman, G.; Friedman, G.; Fridman, A. Physical and Biological Mechanisms of Direct Plasma Interaction with Living Tissue. *New J. Phys.* **2009**, *11*, 115020. [[CrossRef](#)]
23. Wan, J.; Coventry, J.; Swiergon, P.; Sanguansri, P.; Versteeg, C. Advances in Innovative Processing Technologies for Microbial Inactivation and Enhancement of Food Safety—Pulsed Electric Field and Low-Temperature Plasma. *Trends Food Sci. Technol.* **2009**, *20*, 414–424. [[CrossRef](#)]
24. Ehlbeck, J.; Schnabel, U.; Polak, M.; Winter, J.; von Woedtke, T.; Brandenburg, R.; von dem Hagen, T.; Weltmann, K.-D. Low Temperature Atmospheric Pressure Plasma Sources for Microbial Decontamination. *J. Phys. D Appl. Phys.* **2010**, *44*, 013002. [[CrossRef](#)]
25. Kvam, E.; Davis, B.; Mondello, F.; Garner, A.L. Nonthermal Atmospheric Plasma Rapidly Disinfects Multidrug-Resistant Microbes by Inducing Cell Surface Damage. *Antimicrob. Agents Chemother.* **2012**, *56*, 2028–2036. [[CrossRef](#)] [[PubMed](#)]
26. Scholtz, V.; Pazlarova, J.; Souskova, H.; Khun, J.; Julak, J. Nonthermal Plasma—A Tool for Decontamination and Disinfection. *Biotechnol. Adv.* **2015**, *33*, 1108–1119. [[CrossRef](#)]
27. Imlay, J.A. The Molecular Mechanisms and Physiological Consequences of Oxidative Stress: Lessons from a Model Bacterium. *Nat. Rev. Microbiol.* **2013**, *11*, 443–454. [[CrossRef](#)] [[PubMed](#)]
28. Joshi, S.G.; Cooper, M.; Yost, A.; Paff, M.; Ercan, U.K.; Fridman, G.; Friedman, G.; Fridman, A.; Brooks, A.D. Nonthermal Dielectric-Barrier Discharge Plasma-Induced Inactivation Involves Oxidative DNA Damage and Membrane Lipid Peroxidation in *Escherichia coli*. *Antimicrob. Agents Chemother.* **2011**, *55*, 1053–1062. [[CrossRef](#)] [[PubMed](#)]
29. Fang, F.C. Antimicrobial Reactive Oxygen and Nitrogen Species: Concepts and Controversies. *Nat. Rev. Microbiol.* **2004**, *2*, 820–832. [[CrossRef](#)]
30. Šimek, M.; Pekárek, S.; Prukner, V. Ozone Production Using a Power Modulated Surface Dielectric Barrier Discharge in Dry Synthetic Air. *Plasma Chem. Plasma Process.* **2012**, *32*, 743–754. [[CrossRef](#)]
31. Mai-Prochnow, A.; Murphy, A.B.; McLean, K.M.; Kong, M.G.; Ostrikov, K. (Ken) Atmospheric Pressure Plasmas: Infection Control and Bacterial Responses. *Int. J. Antimicrob. Agents* **2014**, *43*, 508–517. [[CrossRef](#)]
32. Doležalová, E.; Prukner, V.; Lukeš, P.; Šimek, M. Stress Response of *Escherichia coli* Induced by Surface Streamer Discharge in Humid Air. *J. Phys. D Appl. Phys.* **2016**, *49*, 075401. [[CrossRef](#)]
33. Graves, D.B. The Emerging Role of Reactive Oxygen and Nitrogen Species in Redox Biology and Some Implications for Plasma Applications to Medicine and Biology. *J. Phys. D Appl. Phys.* **2012**, *45*, 263001–263042. [[CrossRef](#)]
34. Pavlovich, M.J.; Clark, D.S.; Graves, D.B. Quantification of Air Plasma Chemistry for Surface Disinfection. *Plasma Sources Sci. Technol.* **2014**, *23*, 065036. [[CrossRef](#)]
35. Jeong, J.; Kim, J.Y.; Yoon, J. The Role of Reactive Oxygen Species in the Electrochemical Inactivation of Microorganisms. *Environ. Sci. Technol.* **2006**, *40*, 6117–6122. [[CrossRef](#)]
36. Frederickson Matika, D.E.; Loake, G.J. Redox Regulation in Plant Immune Function. *Antioxid. Redox Signal.* **2014**, *21*, 1373–1388. [[CrossRef](#)]
37. Yu, H.; Perni, S.; Shi, J.J.; Wang, D.Z.; Kong, M.G.; Shama, G. Effects of Cell Surface Loading and Phase of Growth in Cold Atmospheric Gas Plasma Inactivation of *Escherichia coli* K12. *J. Appl. Microbiol.* **2006**, *101*, 1323–1330. [[CrossRef](#)] [[PubMed](#)]
38. Sakiyama, Y.; Graves, D.B.; Chang, H.-W.; Shimizu, T.; Morfill, G.E. Plasma Chemistry Model of Surface Microdischarge in Humid Air and Dynamics of Reactive Neutral Species. *J. Phys. D Appl. Phys.* **2012**, *45*, 425201. [[CrossRef](#)]
39. Machala, Z.; Tarabova, B.; Hensel, K.; Spetlikova, E.; Sikurova, L.; Lukes, P. Formation of ROS and RNS in Water Electro-Sprayed through Transient Spark Discharge in Air and Their Bactericidal Effects. *Plasma Process. Polym.* **2013**, *10*, 649–659. [[CrossRef](#)]
40. Montie, T.C.; Kelly-Wintenberg, K.; Roth, J.R. An Overview of Research Using the One Atmosphere Uniform Glow Discharge Plasma (OAUGDP) for Sterilization of Surfaces and Materials. *IEEE Trans. Plasma Sci.* **2000**, *28*, 41–50. [[CrossRef](#)]
41. Sykes, P. Introduction to Organic and Biochemistry. *Biochem. Educ.* **1973**, *1*, 59. [[CrossRef](#)]
42. Mittler, R. ROS Are Good. *Trends Plant Sci.* **2017**, *22*, 11–19. [[CrossRef](#)]
43. Mittler, R.; Vanderauwera, S.; Gollery, M.; Van Breusegem, F. Reactive Oxygen Gene Network of Plants. *Trends Plant Sci.* **2004**, *9*, 490–498. [[CrossRef](#)]
44. Erpen, L.; Devi, H.S.; Grosser, J.W.; Dutt, M. Potential Use of the DREB/ERF, MYB, NAC and WRKY Transcription Factors to Improve Abiotic and Biotic Stress in Transgenic Plants. *Plant Cell. Tissue Organ Cult.* **2018**, *132*, 1–25. [[CrossRef](#)]
45. Hoang, X.L.T.; Nhi, D.N.H.; Thu, N.B.A.; Thao, N.P.; Tran, L.-S.P. Transcription Factors and Their Roles in Signal Transduction in Plants under Abiotic Stresses. *Curr. Genom.* **2017**, *18*, 483–497. [[CrossRef](#)]

46. Seo, E.; Choi, D. Functional Studies of Transcription Factors Involved in Plant Defenses in the Genomics Era. *Brief. Funct. Genom.* **2015**, *14*, 260–267. [[CrossRef](#)] [[PubMed](#)]
47. Iranbakhsh, A.; Ghoranneviss, M.; Oraghi Ardebili, Z.; Oraghi Ardebili, N.; Hesami Tackallou, S.; Nikmaram, H. Non-Thermal Plasma Modified Growth and Physiology in Triticum Aestivum via Generated Signaling Molecules and UV Radiation. *Biol. Plant.* **2017**, *61*, 702–708. [[CrossRef](#)]
48. Jain, D.; Khurana, J.P. Role of Pathogenesis-Related (PR) Proteins in Plant Defense Mechanism. In *Molecular Aspects of Plant-Pathogen Interaction*; Singh, A., Singh, I., Eds.; Springer: Singapore, 2018; pp. 265–281. [[CrossRef](#)]
49. Noctor, G.; Lelarge-Trouverie, C.; Mhamdi, A. The Metabolomics of Oxidative Stress. *Phytochemistry* **2015**, *112*, 33–53. [[CrossRef](#)] [[PubMed](#)]
50. Moon, U.R.; Mitra, A. A Mechanistic Insight into Hydrogen Peroxide-Mediated Elicitation of Bioactive Xanthenes in Hoppea Fastigiata Shoot Cultures. *Planta* **2016**, *244*, 259–274. [[CrossRef](#)] [[PubMed](#)]
51. Filatova, I.; Lyushkevich, V.; Goncharik, S.; Zhukovsky, A.; Krupenko, N.; Kalatskaja, J. The Effect of Low-Pressure Plasma Treatment of Seeds on the Plant Resistance to Pathogens and Crop Yields. *J. Phys. D Appl. Phys.* **2020**, *53*, 244001. [[CrossRef](#)]
52. Kamgang-Youbi, G.; Herry, J.M.; Brisset, J.L.; Bellon-Fontaine, M.N.; Doubla, A.; Naitali, M. Impact on Disinfection Efficiency of Cell Load and of Planktonic/Adherent/ Detached State: Case of Hafnia Alvei Inactivation by Plasma Activated Water. *Appl. Microbiol. Biotechnol.* **2008**, *81*, 449–457. [[CrossRef](#)]
53. Hoeben, W.F.L.M.; van Ooij, P.P.; Schram, D.C.; Huiskamp, T.; Pemen, A.J.M.; Lukeš, P. On the Possibilities of Straightforward Characterization of Plasma Activated Water. *Plasma Chem. Plasma Process.* **2019**, *39*, 597–626. [[CrossRef](#)]
54. Sergeichev, K.F.; Lukina, N.A.; Sarimov, R.M.; Smirnov, I.G.; Simakin, A.V.; Dorokhov, A.S.; Gudkov, S.V. Physicochemical Properties of Pure Water Treated by Pure Argon Plasma Jet Generated by Microwave Discharge in Opened Atmosphere. *Front. Phys.* **2021**, *8*, 596. [[CrossRef](#)]
55. Zhou, R.; Zhou, R.; Prasad, K.; Fang, Z.; Speight, R.; Bazaka, K.; Ostrikov, K. Cold Atmospheric Plasma Activated Water as a Prospective Disinfectant: The Crucial Role of Peroxynitrite. *Green Chem.* **2018**, *20*, 5276–5284. [[CrossRef](#)]
56. Guo, J.; Huang, K.; Wang, X.; Lyu, C.; Yang, N.; Li, Y.; Wang, J. Inactivation of Yeast on Grapes by Plasma-Activated Water and Its Effects on Quality Attributes. *J. Food Prot.* **2017**, *80*, 225–230. [[CrossRef](#)]
57. Guo, J.; Wang, J.; Xie, H.; Jiang, J.; Li, C.; Li, W.; Li, L.; Liu, X.; Lin, F. Inactivation Effects of Plasma-Activated Water on *Fusarium graminearum*. *Food Control* **2022**, *134*, 108683. [[CrossRef](#)]
58. Perez, S.M.; Biondi, E.; Laurita, R.; Proto, M.; Sarti, F.; Gherardi, M.; Bertaccini, A.; Colombo, V. Plasma Activated Water as Resistance Inducer against Bacterial Leaf Spot of Tomato. *PLoS ONE* **2019**, *14*, e0217788. [[CrossRef](#)]
59. Adhikari, B.; Adhikari, M.; Ghimire, B.; Park, G.; Choi, E.H. Cold Atmospheric Plasma-Activated Water Irrigation Induces Defense Hormone and Gene Expression in Tomato Seedlings. *Sci. Rep.* **2019**, *9*, 16080. [[CrossRef](#)] [[PubMed](#)]
60. Danilejko, Y.K.; Belov, S.V.; Egorov, A.B.; Lukanin, V.I.; Sidorov, V.A.; Apasheva, L.M.; Dushkov, V.Y.; Budnik, M.I.; Belyakov, A.M.; Kulik, K.N.; et al. Increase of Productivity and Neutralization of Pathological Processes in Plants of Grain and Fruit Crops with the Help of Aqueous Solutions Activated by Plasma of High-Frequency Glow Discharge. *Plants* **2021**, *10*, 2161. [[CrossRef](#)]
61. ten Bosch, L.; Köhler, R.; Ortman, R.; Wieneke, S.; Viöl, W. Insecticidal Effects of Plasma Treated Water. *Int. J. Environ. Res. Public Health* **2017**, *14*, 1460. [[CrossRef](#)]
62. Zhang, Q.; Ma, R.; Tian, Y.; Su, B.; Wang, K.; Yu, S.; Zhang, J.; Fang, J. Sterilization Efficiency of a Novel Electrochemical Disinfectant against *Staphylococcus Aureus*. *Environ. Sci. Technol.* **2016**, *50*, 3184–3192. [[CrossRef](#)]
63. Tarabová, B.; Lukeš, P.; Hammer, M.U.; Jablonowski, H.; Von Woedtke, T.; Reuter, S.; Machala, Z. Fluorescence Measurements of Peroxynitrite/Peroxynitrous Acid in Cold Air Plasma Treated Aqueous Solutions. *Phys. Chem. Chem. Phys.* **2019**, *21*, 8883–8896. [[CrossRef](#)]
64. Aboubakr, H.A.; Gangal, U.; Youssef, M.M.; Goyal, S.M.; Bruggeman, P.J. Inactivation of Virus in Solution by Cold Atmospheric Pressure Plasma: Identification of Chemical Inactivation Pathways. *J. Phys. D Appl. Phys.* **2016**, *49*, 204001. [[CrossRef](#)]
65. Pavlovich, M.J.; Chang, H.W.; Sakiyama, Y.; Clark, D.S.; Graves, D.B. Ozone Correlates with Antibacterial Effects from Indirect Air Dielectric Barrier Discharge Treatment of Water. *J. Phys. D Appl. Phys.* **2013**, *46*, 015202. [[CrossRef](#)]
66. Fang, J.; Ma, R.; Wang, K.; Tian, Y.; Wang, G.; Zhang, J. Non-Thermal Plasma-Activated Water Inactivation of Food-Borne Pathogen on Fresh Produce. *J. Hazard. Mater.* **2015**, *300*, 643–651. [[CrossRef](#)]
67. Mai-Prochnow, A.; Zhou, R.; Zhang, T.; Ostrikov, K.; Mugunthan, S.; Rice, S.A.; Cullen, P.J. Interactions of Plasma-Activated Water with Biofilms: Inactivation, Dispersal Effects and Mechanisms of Action. *NPJ Biofilms Microbiomes* **2021**, *7*, 1–12. [[CrossRef](#)] [[PubMed](#)]
68. Chen, T.-P.; Su, T.-L.; Liang, J. Plasma-Activated Solutions for Bacteria and Biofilm Inactivation. *Curr. Bioact. Compd.* **2016**, *13*, 59–65. [[CrossRef](#)]
69. Zhou, R.; Zhou, R.; Wang, P.; Luan, B.; Zhang, X.; Fang, Z.; Xian, Y.; Lu, X.; Ostrikov, K.K.; Bazaka, K. Microplasma Bubbles: Reactive Vehicles for Biofilm Dispersal. *ACS Appl. Mater. Interfaces* **2019**, *11*, 20660–20669. [[CrossRef](#)]
70. Jiao, Y.; Tay, F.R.; Niu, L.; Chen, J. Advancing Antimicrobial Strategies for Managing Oral Biofilm Infections. *Int. J. Oral Sci.* **2019**, *11*, 28. [[CrossRef](#)]
71. Cherny, K.E.; Sauer, K. Untethering and Degradation of the Polysaccharide Matrix Are Essential Steps in the Dispersion Response of *Pseudomonas Aeruginosa* Biofilms. *J. Bacteriol.* **2020**, *202*, e00575-19. [[CrossRef](#)]

72. Glazebrook, J. Contrasting Mechanisms of Defense Against Biotrophic and Necrotrophic Pathogens. *Annu. Rev. Phytopathol.* **2005**, *43*, 205–227. [[CrossRef](#)]
73. Grinberg, M.A.; Gudkov, S.V.; Balalaeva, I.V.; Gromova, E.; Sinitsyna, Y.; Sukhov, V.; Vodeneev, V. Effect of Chronic β -Radiation on Long-Distance Electrical Signals in Wheat and Their Role in Adaptation to Heat Stress. *Environ. Exp. Bot.* **2021**, *184*, 104378. [[CrossRef](#)]
74. Voráč, J.; Synek, P.; Procházka, V.; Hoder, T. State-by-State Emission Spectra Fitting for Non-Equilibrium Plasmas: OH Spectra of Surface Barrier Discharge at Argon/Water Interface. *J. Phys. D Appl. Phys.* **2017**, *50*, 294002. [[CrossRef](#)]
75. Voráč, J.; Synek, P.; Potočnáková, L.; Hnilica, J.; Kudrle, V. Batch Processing of Overlapping Molecular Spectra as a Tool for Spatio-Temporal Diagnostics of Power Modulated Microwave Plasma Jet. *Plasma Sources Sci. Technol.* **2017**, *26*, 025010. [[CrossRef](#)]
76. Voráč, J.; Kusýn, L.; Synek, P. Deducing Rotational Quantum-State Distributions from Overlapping Molecular Spectra. *Rev. Sci. Instrum.* **2019**, *90*, 123102. [[CrossRef](#)] [[PubMed](#)]
77. Giampetruzzi, A.; Saponari, M.; Loconsole, G.; Boscia, D.; Savino, V.N.; Almeida, R.P.P.; Zicca, S.; Landa, B.B.; Chacón-Díaz, C.; Saldarelli, P. Genome-Wide Analysis Provides Evidence on the Genetic Relatedness of the Emergent *Xylella fastidiosa* Genotype in Italy to Isolates from Central America. *Phytopathology* **2017**, *107*, 816–827. [[CrossRef](#)] [[PubMed](#)]
78. Goldman, E.; Green, L.H. (Eds.) *Practical Handbook of Microbiology, Second Edition*; CRC Press, Taylor and Francis Group: Boca Raton, FL, USA, 2008.
79. Breed, R.S.; Dotterrer, W.D. The Number of Colonies Allowable On Satisfactory Agar Plates. *J. Bacteriol.* **1916**, *1*, 321–331. [[CrossRef](#)] [[PubMed](#)]
80. Dilecce, G.; Ambrico, P.F.; De Benedictis, S. New $N_2(C^3\Pi_u, v)$ Collision Quenching and Vibrational Relaxation Rate Constants: 2. PG Emission Diagnostics of High-Pressure Discharges. *Plasma Sources Sci. Technol.* **2007**, *16*, S45–S51. [[CrossRef](#)]
81. Dilecce, G. Optical Spectroscopy Diagnostics of Discharges at Atmospheric Pressure. *Plasma Sources Sci. Technol.* **2014**, *23*, 015011. [[CrossRef](#)]
82. Fernández, R.O.; Pizarro, R.A. Lethal Effect Induced in *Pseudomonas Aeruginosa* Exposed to Ultraviolet-A Radiation. *Photochem. Photobiol.* **1996**, *64*, 334–339. [[CrossRef](#)]
83. Kvam, E.; Benner, K. Mechanistic Insights into UV-A Mediated Bacterial Disinfection via Endogenous Photosensitizers. *J. Photochem. Photobiol. B Biol.* **2020**, *209*, 111899. [[CrossRef](#)]
84. Casadesús, J.; Low, D. Epigenetic Gene Regulation in the Bacterial World. *Microbiol. Mol. Biol. Rev.* **2006**, *70*, 830–856. [[CrossRef](#)]
85. Cortese, E.; Settini, A.G.; Pettenuzzo, S.; Cappellin, L.; Galenda, A.; Famengo, A.; Dabalà, M.; Antoni, V.; Navazio, L. Plasma-Activated Water Triggers Rapid and Sustained Cytosolic Ca^{2+} Elevations in *Arabidopsis Thaliana*. *Plants* **2021**, *10*, 2516. [[CrossRef](#)]
86. Soni, A.; Choi, J.; Brightwell, G. Plasma-Activated Water (PAW) as a Disinfection Technology for Bacterial Inactivation with a Focus on Fruit and Vegetables. *Foods* **2021**, *10*, 166. [[CrossRef](#)] [[PubMed](#)]